ARTICLES

Rapid Vibrational Quenching of CO(V) by H_2O and C_2H_2

Baoshan Wang and Yueshu Gu

School of Chemistry, Shandong University, Jinan, Shandong 250100, China

Fanao Kong*

Institute of Chemistry, Chinese Academy of Sciences, Beijing 100080, China

Received: December 4, 1998; In Final Form: July 14, 1999

Rapid relaxation of vibrationally excited carbon monoxide molecules by H_2O and C_2H_2 has been studied by time-resolved Fourier transform infrared emission spectroscopy. The CO(v) molecules were prepared by the laser-induced chemical reaction of $CHBr_3$ with O_2. The temporal vibrational populations of CO(v) are deduced from the time-resolved spectra. For H_2O, eight relaxation rate constants of CO($v = 1-8$) are determined to be 1.7 ± 0.1, 3.4 ± 0.3, 6.2 ± 0.6, 8.0 ± 1.0, 9.0 ± 2.0, 12 ± 3, 16 ± 6, and 18 ± 10 ($\times 10^{-13}$ cm^3 molecule^{-1} s^{-1}), respectively. For C_2H_2, three rate constants of CO($v = 1-3$) are deduced to be 2.0 ± 0.1, 6.0 ± 0.5, and 9.4 ± 2.0 ($\times 10^{-13}$ cm^3 molecule^{-1} s^{-1}), respectively. The excited CO(v) molecules possibly transfer their vibrational energy to the ν_2 vibational modes of H_2O or C_2H_2. The rapid relaxation of CO(v) may be caused by many vibrational impacts in a transient hydrogen-bonded complex. Ab initio calulations are carried out for the CO−H_2O and CO−C_2H_2 complexes. Theoretical calculations are also performed for the quenching rate constants based on both SSH theory and the V−V,R model.

I. Introduction

The vibrational−vibrational (V−V) relaxation of gas molecules has been widely studied in the past few decades. The quenching of vibrationally excited small molecules has been noticed considerably because of their importance in chemical lasers and in combustion chemistry.[1,2] Theoretically, V−V energy transfer has been treated as the transition of the dipole moments during colliding by the well-known Schwartz−Slawsky−Herzfeld (SSH) theory,[3] which deals with the colliding collinearly. An exponential repulsive potential between two harmonic oscillators is adapted. Flynn et al.[4] and Dai et al.[5] suggest that V−V energy transfer collisions are long-range interactions that occur through transition dipole−dipole coupling, while the short-range interaction occurring on the repulsive part of the interaction potential is more important for V−T,R energy transfer. This approach has successfully explained the collisional deactivation of several highly excited triatomic molecules.[5]

When the quencher is a hydrogen-containing molecule, the relaxation becomes very fast.[6] The corresponding rate constant is about 1−2 orders of magnitude higher than that by other ordinary quenchers. For example, the effect of H_2O on the vibrational relaxation of $O_2(v = 1)$ is some 10^4 times more efficient than O_2 collision with another O_2 molecule. Another example is that at room temperature, about 10^2 collisions are needed to deexcite CO_2(010) in the CO_2-H_2O collision to the ground state, but the deexcitation requires more than 10^4 collisions when the collision partner H_2O is replaced by another CO_2.[7,8]

The rapid relaxation can be explained in two ways, forming transient hydrogen-bonded complex[9] and efficient V−R energy compensation.[10,11] The excited molecule can be coupled with the hydrides and forms a collision complex undergoing hindered motions in the neighborhood of its equilibrium geometry. The relative translational motion of the collision partners becomes converted to large-amplitude vibrational motion in the complex. Vibrational relaxation of the excited molecule thus occurs with the energy dissipating into various motions in the complex, especially into the low-frequency hydrogen bonding vibration. This mechanism has been successfully used to explain the collision pairs of HCl−H_2O,[12] H_2O-H_2O,[9] and CO−HF,[13] etc.

The vibrational−rotational (V−R) energy transfer is also proposed to play an important role in the relaxation for the H-containing collisional partners.[11] The hydride molecules have large rotational constant, which allows a substantial amount of vibrational energy to be transferred with minimum change in the rotational quantum number. In a number of studies, Simpson[14] and Barker et al.[15] have shown the V−R transfer effect.

In this paper, we report our experimental and theoretical studies on the energy transfer from highly vibrationally excited CO molecules to two hydride partners, H_2O and C_2H_2. It is known that carbon monoxide can form C-attached or O-attached hydrogen bonding complexes with H_2O and C_2H_2 in both an isolated matrix[16] and gaseous phases.[17−20] The geometries of these weakly bonded van der Waals complexes have been well defined through the microwave or far-IR spectroscopy measurements.[17−20]

Stephenson et al.[21] studied the quenching of CO by H_2O using

* Corresponding author.

10.1021/jp984616a CCC: $18.00
Published on Web 08/31/1999

the laser-induced fluorescence (LIF) technique. Only one relaxation rate constant for CO($v = 1 \rightarrow 0$) was obtained. In the present work, eight relaxation rate constants of CO($v = 1-8$) by H_2O and three relaxation rate constants of CO($v = 1-3$) by C_2H_2 were obtained. The experiment was performed with time-resolved Fourier transform infrared spectroscopy (TR FTIR). An ab initio molecular orbital calculation was carried out to understand the geometries and energetics for the CO−H_2O and CO−C_2H_2 complexes. Finally, the SSH theory and the V−V,R model[22,23] have been used to calculate the quenching rate constant of CO(v) and compared with the experimental data.

II. Experimental Section

The experimental apparatus has been described in detail elsewhere.[24] The apparatus consists of an ArF laser (100mJ, Lambda Physik-305i), a reaction chamber, and a time-resolved FTIR spectrometer (Nicolet 800). The 193 nm laser was used to initiate the photochemical reaction of $CHBr_3$ and O_2, which has been proven to be an efficient method to generate the highly vibrationally excited CO(v) molecules. The O_2 gas carried the vapor of liquid $CHBr_3$ (Baker reagent, not further purified) into the vacuum chamber. The flow rate of the reactant gases was controlled by flowmeters. The partial pressure of $CHBr_3$ was estimated to be 5 Pa in the chamber. The partial pressure of O_2 was maintained at 15 Pa. 50 Pa H_2O vapor or 65 Pa C_2H_2 gas were introduced to the chamber for the CO/H_2O or CO/C_2H_2 system, respectively. A pair of large gold-coated White cell mirrors (nearly confocal) were used to collect the IR fluorescence. The IR emission was collimated to the FTIR spectrometer, which was operated in a rapid scan mode. The spectral resolution was set at 16 cm^{-1}. To improve the signal-to-noise ratio, the interferogram data were coadded for 20 times and then Fourier transformed to the IR spectrum.

The sequential time-resolved infrared emission spectra with a time uncertainty of 5 μs were recorded. Contributions to IR intensities due to instrumental spectral response, background radiation, and absorptions of water vapor and carbon dioxide were corrected for.

III. Results and Discussion

1. Preparation of CO(v) Molecules. The CO(v) molecules were prepared by the laser-induced chemical reaction of $CHBr_3$ and O_2 in the gas phase. The detailed mechanism is not clear. But it is believed that the focused UV laser beam initiates a two-photon photodissociation of the precursor molecule $CHBr_3$, generating CH radical. The later species react with the oxygen fiercely. The reaction is exothermic, producing vibrationally hot CO($v \leq 14$) molecules.[25]

It is estimated that about 1% $CHBr_3$ in the photolysis zone ($10 \times 5 \times 5$ cm^3) was dissociated, and the density of the vibrationally hot CO(v) was about 10^{13} molecules/cm^3, which was sufficient to be detected by the FTIR spectrometer. Less than 1% of the CO($v \rightarrow v - 1$) emission was self-absorbed by the rest of the CO(v) moelcules in the reaction zone.

It took about 100 μs to complete the CO(v) producing reaction in the present gas pressure. To investigate the relaxation kinetics of CO, we recorded the IR spectra starting from 160 μs after the laser firing.

2. Relaxation of CO(v) by H_2O. The vibrational relaxation of the excited CO(v) molecules quenched by water vapor was experimentally investigated. The relaxation process was traced by the evolution of CO($v \rightarrow v - 1$) emission spectra. Starting at the delay time of 160 μs after the laser firing, 15 sequential IR emission spectra with intervals of 50 μs each were recorded and shown in Figure 1.

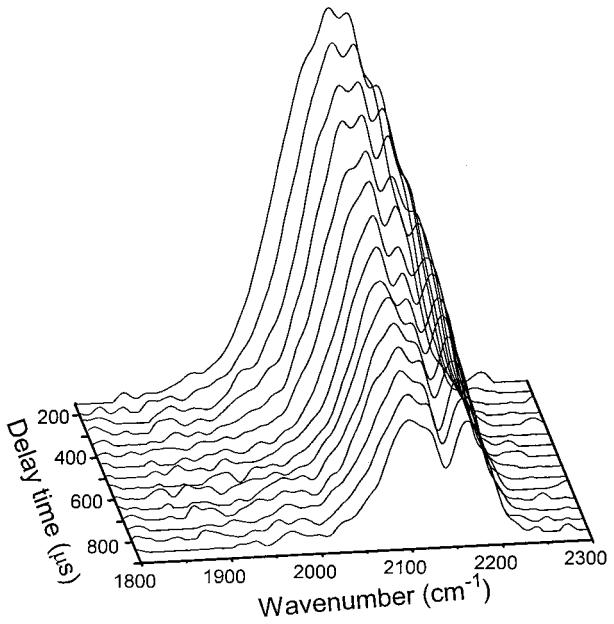

Figure 1. Time-resolved infrared emission spectra of CO($v \rightarrow v - 1$) quenched by H_2O. A gas mixture of 5 Pa $CHBr_3$/15 Pa O_2/50 Pa H_2O was used.

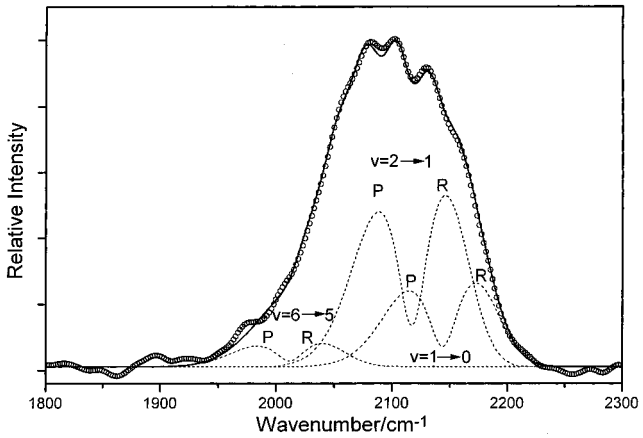

Figure 2. A typical experimental (circles) and the simulated (solid line) spectrum of the CO($v \rightarrow v - 1$) emission for the CO/H_2O system at a delay time of 260 μs. The contributions of some transitions to the simulated spectra are shown by dashed lines.

For each spectrum, a simulation is made to determine the transient vibrational population of CO(v). The detailed simulation process is described in a previous paper.[24] In the simulation, the rotational temperature of CO(v) is assumed to be 300 K. As an example, a typical simulated spectrum at the delay time of 260 μs is shown in Figure 2. The spectral envelope of the emission is composed by P and R branches of individual rovibrational bands. For clarity, only the contributions from three vibrational transitions are drawn in the figure with dashed lines. From the best-fit simulations, a set of transient vibrational population of CO(v) is found. A standard deviation of 5%−10% is estimated for the population, leading to a 10%−30% deviation of the quenching rate constants.

At a gaseous pressure of 70 Pa, the average free path L of a CO molecule is about 90 μm at 300 K. Within 1 ms, the molecule will collide for about $Z = 7000$ times and the diffusion distance $D = Z^{1/2}L$ is only 0.8 cm. That means the IR luminescent zone will expand 0.8 cm in each direction from its

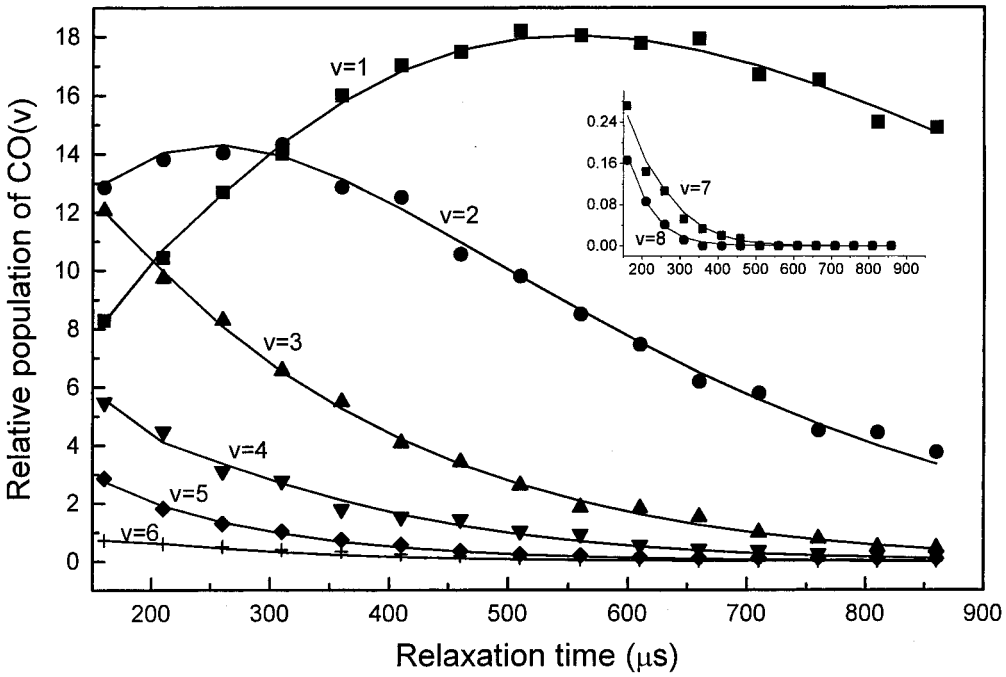

Figure 3. Vibrational population of CO(v) at different delay times for the CO/H_2O system. The dots represent experimental data obtained by the spectral simulation. The solid lines are evaluated from the relaxation equations. The insert shows the populations of $v = 7,8$.

photolysis area of $5 \times 5 \times 10$ cm^3. But it still much less than the light collection zone of $10 \times 10 \times 20$ cm^3. Therefore, the diffusion effect was ignored in our evaluation. The rate constant may be overestimated at most by 10%.

The transient populations at the 15 different delay times are shown in Figure 3. It can be seen in the figure that the population of high vibrational levels ($v > 3$) decays monotonically with time. However, for the levels $v = 1$ and $v = 2$, the population increases before 600 μs and 250 μs, respectively, then decreases.

With the obtained time-dependent vibrational populations, the quenching rate constants of CO(v) are calculated by solving the master equations:

$$dn_v/dt = (\sum k_{v+1,i}[M_i] + A_{v+1})n_{v+1} - (\sum k_{v,i}[M_i] + A_v)n_v, \quad v = 1,2,\ldots, N \quad (1)$$

where n_v is the population of the vth vibrational level, $k_{v,i}$ is the relaxation rate constant of the level v quenched by M_i species, $[M_i]$ is the number density of the collisional partner M_i, A_v is the Einstein spontaneous emission coefficient of the level v, and N represents the highest vibrational level to be considered.

The rate equations 1 are numerically solved by the differential method we have suggested. Eight quenching rate constants k_v-($v = 1-8$) of CO(v) by H_2O were obtained and listed in Table 1. The best-fit curves were also shown in Figure 3.

The first quenching rate constant $k_1 = (1.7 \pm 0.1) \times 10^{-13}$ cm^3 molecule^{-1} s^{-1} is close to Stephenson's result,[21] 2.0×10^{-13} cm^3 molecule^{-1} s^{-1}. The k_v increases with the vibrational quantum number v. Figure 4 shows a linear relationship between log k_v and log v. Comparing to the empirical formula

$$k_v = v^n k_1 \quad (2)$$

the slope n is 1.0.

As illustrated in Figure 5, among the three vibrational modes ($\nu_1 = 3651.7$ cm^{-1}, $\nu_2 = 1595.0$ cm^{-1}, and $\nu_3 = 3755.8$ cm^{-1}) of water molecule, the ν_2 mode of H_2O has a minimum energy defect ΔE with that of carbon monoxide and becomes the most feasible channel. The higher the vibrational level of CO(v), the smaller the energy defect ΔE with $H_2O(010)$, and thus the greater the relaxation rate. Unfortunately, the emission of H_2O-(010→000) transition could not be observed in our experiment

TABLE 1: Vibrational Quenching Rate Constants (in 10^{-13} cm^3 molecule^{-1} s^{-1}) of CO(v) by H_2O and by C_2H_2

	quencher H_2O			quencher C_2H_2		
CO(v)		SSH	V−V,R		SSH	V−V,R
v	expt	calc	calc	expt	calc	calc
1	1.7 ± 0.1	1.8	2.0	2.0 ± 0.1	0.32	2.1
2	3.4 ± 0.3	3.6	4.0	6.0 ± 0.5	0.64	4.2
3	6.2 ± 0.6	5.4	6.0	9.4 ± 2.0	0.96	6.3
4	8.0 ± 1.0	7.2	8.0			
5	9.0 ± 2.0	9.0	10.0			
6	12 ± 3	10.8	12.0			
7	16 ± 6	12.6	14.0			
8	18 ± 10	14.4	16.0			

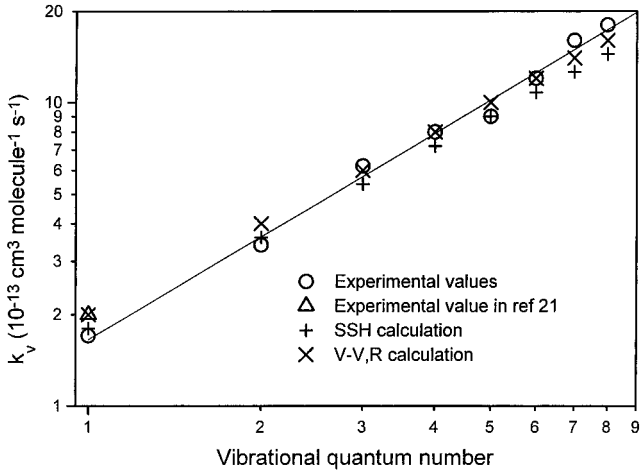

Figure 4. Plot of log k_v vs log v for the quencher H_2O system. The slope of the solid line is 1.0. The SSH and V−V,R theoretical results are also shown in the plot.

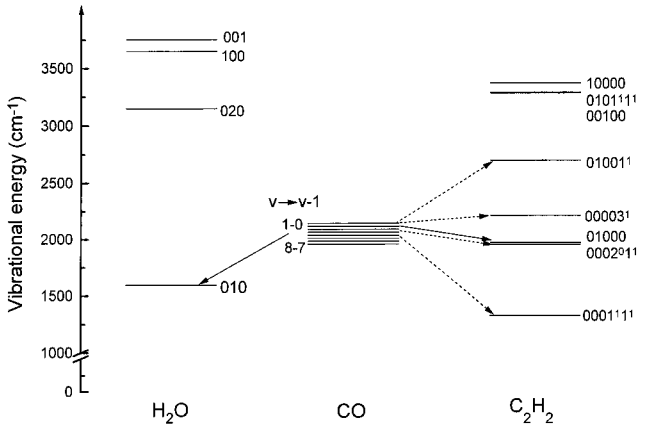

Figure 5. Vibrational energy diagram of CO($v \rightarrow v - 1$) and H_2O and C_2H_2 molecules. The solid arrows show the preferential energy transfer channels. The dashed arrows indicate the possible multiquanta channels.

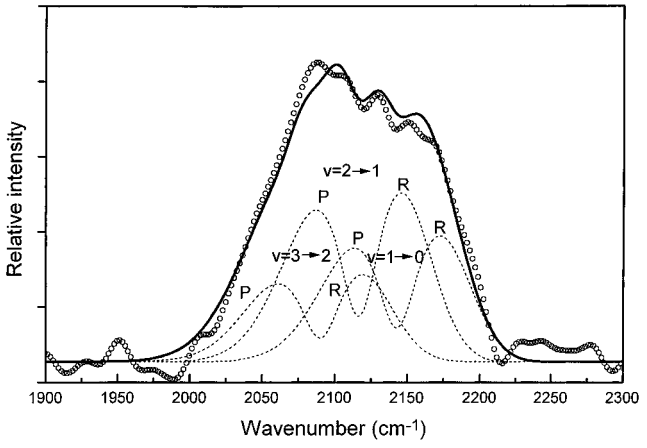

Figure 6. The experimental (circles) and the simulated (solid line) spectrum of the CO($v \rightarrow v - 1$) emission for CO/C_2H_2 system at a delay time of 160 μs. The contributions of some transitions to the simulated spectra are shown by the dashed lines.

because the wavelength is out of the detection range of the InSb detector used.

3. Relaxation of CO(v) by C_2H_2. The quenching of the excited CO(v) molecules by acetylene was also studied. Starting at 160 μs after the laser pulse, 14 sequential spectra with the time intervals of 50 μs were recorded. Each time-resolved spectrum has been simulated to obtain the transient vibrational population of CO(v). The rotational temperature is assumed as 300 K in the simulation. A typical simulated spectrum is shown in Figure 6 in comparison with the experimental data.

Figure 7 shows time evolution of the vibrational population of CO($v = 1-3$). The quenching of the higher vibrational levels ($v > 3$) was too fast in the present experimental condition so that we could not obtain their relative population. The population of $v = 2$ and $v = 3$ decayed monotonically, while that of $v = 1$ accumulated gradually before 300 μs and then decreased slowly.

The relaxation rate equations (eq 1) are also solved by the differential method. Three quenching rate constants of CO($v = 1-3$) by C_2H_2 are obtained and listed in Table 1. The best-fit curves are shown in Figure 7. k_v increases with the vibrational level v. The log k_v also shows a linear relationship to log v (Figure 8), but the slope n is 1.5.

Carbon monoxide is analogous to acetylene, being linear and having a triple bond. Their reduced masses are close. Therefore, the "heavy atom" stretching vibrational frequencies are similar.

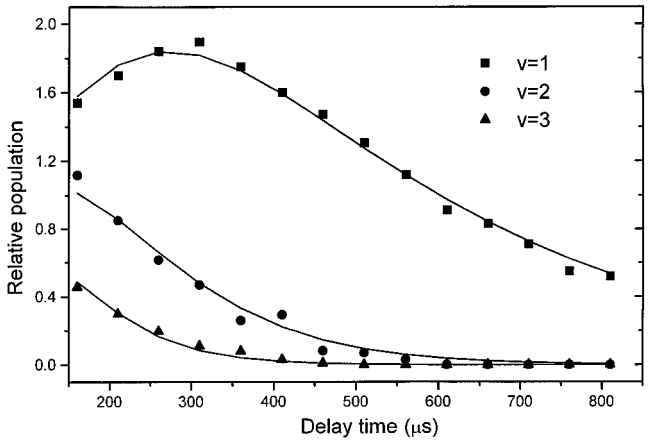

Figure 7. Vibrational population of CO(v) at different delay times for the CO/C_2H_2 system. The dots represent experimental data obtained by the spectral simulation. The solid lines are calculated from the relaxation equations.

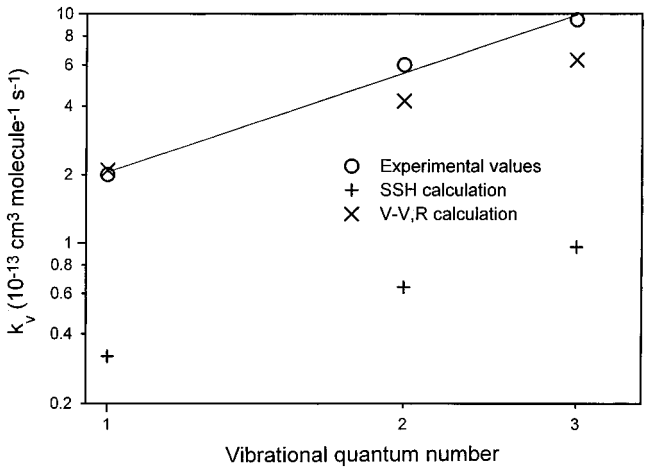

Figure 8. Power law plot of log k_v vs log v for the quencher C_2H_2. The slope of the solid line is 1.5. The calculation results with the SSH and V−V,R theories are also shown for comparison.

The frequencies of CO transitions ($1 \rightarrow 0$, $2 \rightarrow 1$, $3 \rightarrow 2$) are 2143.1, 2116.6, and 2090.2 cm^{-1}, respectively, while that of the ν_2 mode of C_2H_2 is 1973.8 cm^{-1}. The energy discrepancy is only 120−170 cm^{-1}. Therefore, near resonant V−V energy transfer may take place efficiently between the two molecules. The ν_2 mode is IR forbidden throughout, but this restriction may be broken in the C_2H_2−CO complex by strong perturbations. Some other channels with minor contributions to the energy transfer may also occur. In Figure 5, four dashed arrows show that the vibrational energy may transfer to the 00003^1, 0002^01^1, 01001^1, or 0001^11^1 modes of the acetylene molecule. These transitions are multiquanta processes so that the probabilities are much lower than the single quantum process of the ν_2 mode. It is noted that the 01001 states in acetylene could be excited through single-quantum ν_2 excitation of the thermally populated 00001 state.

4. SSH Calculations. The SSH theory[3] is used to calculate the quenching rate constants of CO(v) by H_2O and C_2H_2. Only the single-quantum V−V process is considered in our SSH calculation. The parameters used in the calculation are listed in Table 2. The calculated rate constants for all the vibrational levels are collected in Table 1. The results are also shown in the log k_v−log v plots (Figure 4 and Figure 8). The SSH theory is a crude model with some simplified approximations. The calculated results strongly depend on the parameters used, especially the Lennard-Jones potential well (ϵ) and radii (σ).

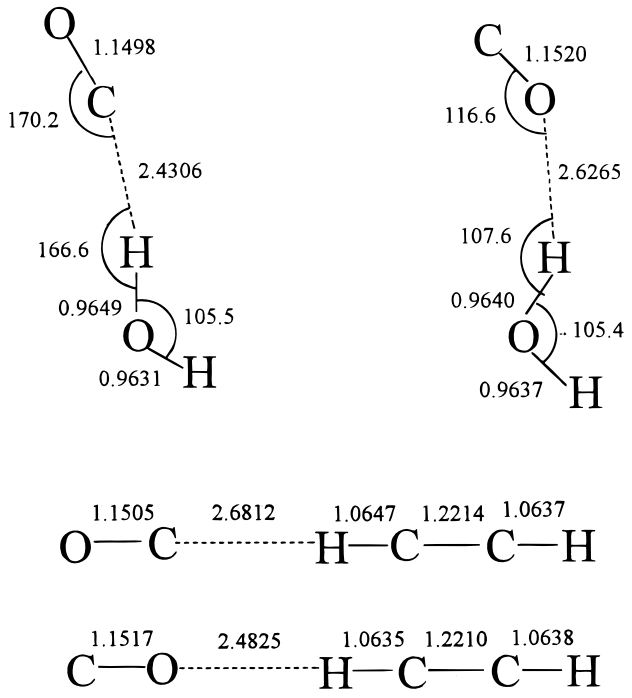

Figure 9. RMP2/6-31++G(d,p) optimized structures of the CO−H_2O and CO−C_2H_2 complex. Bond lengths are in angstroms, and bond angles are in degrees.

TABLE 2: Parameters Used in the SSH Theoretical Calculation

					Lennard-Jones parameter	
molecule	ω_e (cm^{-1})	$\omega_e x_e$ (cm^{-1})	A^2 (amu^{-1})	steric factor	ϵ (K)	σ (Å)
CO	2169.6	13.3	0.017	1/3	105	3.70[a]
H_2O	1595.0		0.9527	2/3	506	2.71[a]
C_2H_2	1973.8		0.063	1/3	186	4.22[b]

[a] Reference 27. [b] Reference 28.

Unfortunately, the calculated ϵ and σ values in the publications are diverse, resulting in large discrepancy between the SSH calculated and the experimental rate constants. In some case, the discrepancy is as large as one or 2 orders of magnitude. Our SSH calculations on the CO/H_2O system are in good agreement with the experimental values. However, for the CO(v)/C_2H_2 system, the calculated rate constants are about 1 order of magnitude lower than the experimental data.

The dissatisfication with the uncertainty of the SSH computation results invokes a more precise theoretical calculation. The V−V,R model[22] is applied to calculate the energy transfer in the hydrogen-bonded complexes.

5. CO−H_2O and CO−C_2H_2 Complexes. Carbon monoxide molecule can form hydrogen bonded complex with H_2O or C_2H_2 molecules. The monomer in the complex vibrates and repeats many impacts to the neighboring molecule before the complex dissociates.

To gain an insight into the geometries and the energetics of the complexes, and to provide necessary data for the later calculation with the V−V,R model, ab initio computation has been performed to investigate the CO−H_2O and CO−C_2H_2 complexes using the Gaussian 94 program.[26] Structures of the complexes are optimized via the supermolecular Moller−Plesset perturbation theory to the second order within the close-shell frozen-core approximation (RMP2=FC) with the basis set 6-31++G(d,p). The harmonic frequencies are calculated at the same level. Single-point calculations based on the MP2 geometries are also performed at the RCCSD(T) level with a larger basis set 6-31++G(2d,2p). Two types of the complexes, referring to the hydrogen atom attached to the C atom of CO and H attached to the O atom of CO, are optimized and shown in Figure 9. Some related properties are listed in Tables 3 and 4 for CO/H_2O and CO/C_2H_2, respectively. The calculated results are in good agreement with the available experimental data,[16−20] which are also listed in the tables. Both our calculations and the previously calculated results indicate that the complexes of the C−H hydrogen bond are more stable than that of the O−H hydrogen bond. The binding energies for the OC−H_2O and OC−C_2H_2 complexes are estimated to both be about 3.0 kJ/mol.

TABLE 3: Selected Properities of the CO−H_2O Complexes[a]

complex	OC−HOH	CO−HOH
geometry	R_{CH}: 2.43 (2.41) θ_{CHO}: 13.4 (11.5)	R_{CH}: 2.63 θ_{OHO}: 72.4
ω (cm^{-1})	52.3, 66.4, 97.2, 197.2,[b] 316.4, 2120.6, 1623.9, 3852.4, 3998.0	28.7, 86.7, 92.4, 140.1, 141.7,[b] 2105.4, 1620.5, 3856.8, 4002.7
$\Delta\omega$ (cm^{-1})[c]	12.3, 4.3, −11.0, −12.2	−1.9, 0.9, −6.6, −7.5
$\Delta\omega_{expt}$[d]	10.6, 5.4, −8.8, −9.5	
k_s (mdyn/Å)[e]	0.0274 (0.0274)	0.0155
I (g/mol $Å^2$)[f]	1.0, 184.3, 185.2 (184.0)[a]	8.8, 114.5, 123.3
ΔE_0^0 (kJ/mol)[g]	−3.07	−1.76

[a] The values in parentheses are the experimental results from refs 17 and 18. [b] Hydrogen bonding stretching frequency. [c] Frequency shifts for two monomers vibrational fundamentals. [d] Reference 29. [e] Force constant for the hydrogen bond. [f] Overall moments of inertia. [g] $\Delta E_0^0 = E_{complex} - (E_{CO} + E_{H2O})$ with zero-point energy correction.

TABLE 4: Selected Properities of the CO−C_2H_2 Complexes[a]

complex	OC−HCCH	CO−HCCH
geometry	R_{cm}: 5.014 (5.018, 5.011) θ_{CHC}: 0.0 (0.0)	R_{cm}: 4.688 θ_{OHC}: 0.0
ω (cm^{-1})	38.9, 38.9, 69.9,[b] 96.3, 96.3, 420.4, 770.6, 1981.9, 2114.2, 3480.1, 3568.3	17.6, 17.6, 64.7,[b] 83.7, 83.7, 443.6, 768.1, 1985.0, 2104.9, 3489.5, 3576.4
$\Delta\omega$ (cm^{-1})[c]	6.9, 23.9, 31.1, −2.9, −7.5, −6.5	−2.4, 47.1, 28.6, 0.2, 1.9, 1.6
k_s (mdyn/Å)[d]	0.0253 (0.0171)	0.0217
I (g/mol·$Å^2$)[e]	362.4 (362.0)	315.1
ΔE_0^0 (kJ/mol)[f]	−2.52 (−3.58)	−2.00

[a] The values in parentheses are the experimental results from refs 19 and 20. [b] Hydrogen bonding stretching frequency. [c] Frequency shifts for two monomers vibrational fundamentals. [d] Force constant for the hydrogen bond. [e] Overall moments of inertia. [f] $\Delta E_0^0 = E_{complex} - (E_{CO} + E_{C2H2})$ with zero-point energy correction.

6. The Calculation of the V−V,R Model. Because the hydride monomers have large rotational constants, the vibational energy defect can be efficiently compensated by the change of the rotational quanta of the hydrides. Therefore, V−R energy transfer between CO(v) and H_2O or C_2H_2 can make a considerable contribution.

Sentman[22] suggested a V−V,R model to deal with this kind of energy transfer process. For the $1 \rightarrow 0$ transition of CO(v), the thermal average transition probability is given as

$$\langle P_{10} \rangle = C_v F_v(\omega,B,\mu,\sigma,T) + C_R F_R(\omega,B,\mu,\sigma,T) \qquad (3)$$

The first and the second terms represent the V−V and V−R contributions to the overall deactivation of CO(v), respectively. F_v and F_R are the functions of the vibrational frequency ω, the rotational constant B, the reduced mass μ, the Lennard-Jones potential radii σ, and the temperature T. C_v and C_R are the coefficients defined as $C_v = \gamma_H \sigma^2 \mu_{HX} \omega_{HX}$ and $C_R = \gamma_C/\mu_{CO}\ \omega_{CO}$, where $\gamma_H = m_H/m_{HX}$ and $\gamma_C = m_C/m_{CO}$. The quenching

TABLE 5: Parameters Used in the V−V,R Calculation

complex	ν_s/cm^{-1}	ω/cm^{-1}	bond	R_e/Å	σ/Å
O−C···H−OH	197.2	2143.1	O−C	1.128	3.70
		1595.0	H−O	0.956	2.71
O−C···H−C_2H	70.0	1973.8	H−C	1.058	4.22

rate constants can be obtained by

$$k_v = v\langle P_{10}\rangle \pi d^2 \quad (4)$$

where d is the collisional diameter.

Because the above formulas deal with the interaction between two diatomic molecules, a diatomic approximation[23] is used in our calculation. H_2O and C_2H_2 are treated as H−OH and H−C_2H, respectively. Table 5 lists the parameters used. The calculated quenching rate constants are listed in Table 1 and plotted in Figures 4 and 8. For both the CO/H_2O and the CO/C_2H_2 systems, the calculated k_v's are in reasonable agreement with the experimental values.

The frequent intracomplex collision explains why the energy transfer between CO and the two hydrides takes place so efficiently. It is estimated that about 500 impacts between the two moieties take place before the complex dissociates. Meanwhile, there are approximately 800 gas-kinetic collisions from the time of the excimer laser pulse to the first emission measurement (160 μs). As many as 4000 collisions have occurred for the longest time data (860 μs). It is entirely possible that a fraction of the random gas-kinetic collisions have a similar outcome to the oriented collisions that occur in the complex.

IV. Conclusions

(1) The dynamic process of the vibrational quenching of CO(v) by H_2O and C_2H_2 was detected by TR FTIR spectroscopy.

(2) Eight quenching rate constants for CO(v)/H_2O and three quenching rate constants for CO(v)/C_2H_2 were obtained.

(3) The excited CO(v) possibly transfers its vibrational energy to the ν_2 modes of H_2O or C_2H_2 molecules. In the CO/C_2H_2 system, several multiquanta energy exchange channels may also occur.

(4) The SSH calculation has been carried out for both of the systems. The calculated rate constants of the CO/H_2O system agree the experimental data well. But for the CO/C_2H_2 system, the calculated results are 1 order of magnitude lower than the experimental values.

(5) The geometry and energy of the complexes of CO−H_2O and CO−C_2H_2 were investigated by ab initio calculation. The C-attached complexes are more stable than the O-attached complexes.

(6) The V−V,R model was adapted to calculate the quenching rate constants. The calculated rate constants are in good agreement with the measured data.

Acknowledgment. This work is supported by the National Natural Science Foundation of China. This manuscript was reviewed carefully by Prof. Zhu Qihe.

References and Notes

(1) Flynn, G. W.; Paramenter, C. S.; Wodtke, A. M. *J. Phys. Chem.* **1996**, *100*, 12817.
(2) Flynn, G. W. *Acc. Chem. Res.* **1981**, *14*, 334.
(3) Schawartz, R. N.; Slawsky, Z. I.; Herzfeld, K. F. *J. Chem. Phys.* **1952**, *20*, 1591.
(4) Zhou, J. Z.; Flynn, G. W. *J. Chem. Phys.* **1990**, *93*, 6099.
(5) Hartland, G. V.; Qin, D.; Dai, H.-L. *J. Chem. Phys.* **1997**, *107*, 2890.
(6) Cottrell, T. L.; McCoubreg, J. C. *Molecular Energy Transfer in Gases*; Butterworth: London, 1961; pp 96−97 and 168.
(7) Eucken, A.; Kuchler, L. *Phys. Z.* **1938**, *39*, 831.
(8) Pielemeier, W. H.; Byers, W. H. *J. Acount. Soc. Am.* **1943**, *15*, 17.
(9) Shin, H. K. *J. Chem. Phys.* **1993**, *98*, 1964.
(10) Shin, H. K. *Chem. Phys. Lett.* **1975**, *32*, 218.
(11) Mudjijono; Lawrance, W. D. *J. Chem. Phys.* **1996**, *105*, 3019.
(12) Shin, H. K. *Chem. Phys. Lett.* **1994**, *228*, 678.
(13) Wallis, E. P.; Thompson, D. L. *J. Chem. Phys.* **1992**, *97*, 4929.
(14) Siddles, R. M.; Wilson, G. J.; Simpson, C. J. S. M. *Chem. Phys. Lett.* **1994**, *225*, 146.
(15) Yerram, M. L.; Brenner, J. D.; King, K. D. Barker, J. R. *J. Chem. Phys.* **1990**, *94*, 6341.
(16) Lundell, J.; Rasanen, M. *J. Phys. Chem.* **1995**, *99*, 14301.
(17) Yaron, D.; Peterson, K. I.; Zolandz, D.; Klemperer, W.; Lovas, F. J.; Suenram, R. D. *J. Chem. Phys.* **1990**, *92*, 7095.
(18) Bumarner, R. E.; Suzuki, S.; Stockman, P. A.; Green, P. G.; Blake, G. A. *Chem. Phys. Lett.* **1991**, *176*, 123.
(19) Marshall, M. D.; Prichard, D. G.; Muenter, J. S. *J. Chem. Phys.* **1989**, *90*, 6049.
(20) Roehrig, M. A.; Kukolich, S. G.; *Chem. Phys. Lett.* **1991**, *188*, 232.
(21) Stephenson, J. C.; Mosburg, E. R., Jr. *J. Chem. Phys.* **1974**, *60*, 3562.
(22) Sentaman, L. H. *Chem. Phys. Lett.* **1973**, *18*, 493.
(23) Lieb, S. G.; Bevan, J. W. *Chem. Phys. Lett.* **1985**, *122*, 284.
(24) Wang, B.; Gu, Y.; Kong, F. *J. Phys. Chem. A* **1998**, *102*, 9367.
(25) Lin, M. C. *J. Chem. Phys.* **1974**, *61*, 1835.
(26) Frish, M. J.; Head-Gordon, M.; Trucks, G. W.; Foresman, J. B.; Schlegel, H. B.; Raghavachari, K.; Robb, M. A.; Binkley, J. S.; Gonzales, C.; DeFrees, D. J.; Fox, D. J.; Whiteside, R. A.; Seeger, R.; Melius, C. F.; Baker, J.; Martin, R. L.; Kahn, L. R.; Stewart, J. J. P.; Topiol, S.; Pople, J. A. *Gaussian 94*, revision E.1.; Gaussian, Inc.: Pittsburgh, PA, 1995.
(27) Toselli, B. M.; Brenner, J. D.; Yerram, M. L.; Chin, W. E.; King, K. D.; Barker, J. R. *J. Chem. Phys.* **1991**, *95*, 176.
(28) Calos, M.; Hernando, P.; Juan, F.; Carlos, G.; Eugenio, S. *J. Chem. Phys.* **1983**, *78*, 5971.
(29) Lundell, J.; Latajka, Z. *J. Phys. Chem.* **1997**, *101*, 5004.